

Electrical Conductance of Molecular Junctions by a Robust Statistical Analysis

M. Teresa González*, Songmei Wu, Roman Huber, Sense J. van der Molen,

Christian Schönenberger, and Michel Calame

Institut für Physik, Universität Basel, Klingelbergstr. 82, CH-4056 Basel, Switzerland

March 23, 2022

Abstract

We propose an objective and robust method to extract the electrical conductance of single molecules connected to metal electrodes from a set of measured conductance data. Our method roots in the physics of tunneling and is tested on octanedithiol using mechanically controllable break junctions. The single molecule conductance values can be deduced without the need for data selection.

To determine the feasibility of devices based on single molecules and to assess their properties, a single or a few molecules have to be wired between two metal electrodes. This has become a reality only recently through different techniques such as scanning-probe microscopy, and mechanical and electromigration break junctions.¹⁻⁵ Using these techniques, the electrical conductances G of a broad range of molecular junctions have been determined⁶⁻⁹ and gating of single molecules has been demonstrated.¹⁰⁻¹³

*Email: teresa.gonzalez@unibas.ch Web: <http://www.unibas.ch/phys-meso>

These promising results are somewhat counterbalanced by the poor agreement in the conductance values of single molecules reported by different groups. This disagreement reflects our present poor insight into the atomistics of single molecule junctions. To overcome junction-to-junction fluctuations, a statistical analysis has been proposed, in which G values of many junction realizations are represented in a histogram. This analysis has first been implemented in atomic junctions,^{4,14,15} and has subsequently been used in metal-molecule junctions.^{1,3,6} Peaks in the histogram point to preferred junction geometries. Evidence for the formation of few-molecules junctions was derived from the observation of a series of G values appearing at multiples of a fundamental single molecule value. The appearance of peaks in G -histograms is a very striking observation. However, to resolve these, data selection schemes have been applied.¹⁶⁻¹⁸ This situation is unsatisfactory, because there is at present no generally accepted objective selection criterion. We address this important question in this Letter.

As a test case, we have chosen octanedithiol junctions.^{1,3,17-21} We use a mechanically controllable break junction (MCBJ)^{22,23} setup and acquire many conductance traces in succession. We compare conductance histograms, which were generated with and without data selection. We show that the conductance value assigned to a single molecule is *robust*, and that data selections do not help to improve the results. The most convincing representation is found in a histogram of $\log G$ rather than G .

The measurements were performed at room temperature, in a liquid environment. Figure 1a shows a schematics of our MCBJ setup.²⁴ As flexible substrates, we use electrically isolated stainless steel sheets, over which gold leads are fabricated by electron beam lithography. The scanning-electron microscope (SEM) image in Figure 1a shows the suspended 100 nm-wide region in the center of the gold leads. A flexible cell in the top of the substrate guarantees that the leads are always immersed in liquid, (see Figure 1a). The substrate is held by two supports at the periphery and a push-rod pressing from below. Bending the substrate results in stretching the

suspended Au bridge, which shrinks (b) until it breaks (c) and a gap of size d forms. The change in gap-size Δd is related to the vertical movement of the push-rod Δz by an attenuation factor $a = \Delta d/\Delta z = 1.6 - 4 \times 10^{-5}$.^{24,25} The push-rod is moved at a velocity $v_z = 30 \mu\text{m/s}$, so that the two Au leads separate at $0.5 - 1.2 \text{ nm/s}$.

We apply a constant bias voltage of 0.2 V , and record the variation of the current I through the junction during repeated open-close cycles. The current was measured with a current-voltage converter, which can automatically adjust its gain between 0.1 and $100 \text{ V}/\mu\text{A}$. This allows us to register the conductance variation during the whole process, starting from the fused Au junction with $G > G_0 := 2e^2/h$, until the formation of single molecule junctions, with conductance values orders of magnitude lower.

The formation of a metal-molecule bridge evolves in several steps. First, the Au-bridge gets thinner (Figure 1b), until a rather stable single-atom contact is established. A plateau in the $G(z)$ curve is then expected around G_0 . When the atomic contact is finally lost, the conductance decreases strongly. This decrease may be interrupted if a metal-molecule bridge is formed (Figure 1c). In that case, another plateau in the $G(z)$ curve is anticipated.^{3,26} Similar to atomic junctions, this metal-molecule-metal bridge holds via its chemical bonds the two sides together and postpones the breaking open of the Au electrodes (Figure 1d).

To explore this process, we have performed groups of 100 consecutive open-close cycles for five different samples, both in pure mesitylene, and in a 1 mM solution of octanedithiol in mesitylene. In Figure 2, we show representative $G(z)$ curves during opening of the bridge. Whereas the curves in the main panel focus on values in the low conductance regime, i.e., at $G \approx 10^{-4} G_0$, the inset shows data around $G \approx G_0$, corresponding to the single-gold-atom contact. Figure 2 shows how the shape of the conductance curves $G(z)$ is modified by the presence of octanedithiol molecules. Whereas $G(z)$ decays in an exponential fashion in the pure solvent (curves to the left of the dotted line), distinct plateau features may appear in octanedithiol containing solution. These plateaus are

the signature of the formation of single (few) molecule junctions. In some curves, jumps between plateaus at different G can be seen. In those cases, the molecular junction reorganizes, and the number of bridging molecules may change. In Figure 2, the first two curves (blue) to the right of the vertical dotted line, are rather “clean”. In contrast, the three next curves (red) are quite noisy just before plateau formation. This suggests that there is a large degree of molecular movement in the junction, until the octanedithiol molecules eventually lock between the leads. Finally, some $G(z)$ curves measured in the presence of molecules do not display plateaus (last three curves in green). In this case, no stable single-molecule bridge has been formed. Such traces correspond to approximately 50% of the curves.

Next, we focus on the statistics of our measured data. For each sample, we take all 100 conductance traces $G(z)$, and determine the probability with which a particular G -value is measured, $N_G(G)$. This is depicted in the conductance histograms of Figure 3a (bin size: $\Delta G = 4 \times 10^{-6} G_0$). Whereas $N_G(G)$ decays smoothly in the pure solvent, there are distinct peaks appearing in the octanedithiol case (indicated by arrows). This suggests that particular molecular configurations form with a high probability. However, the peaks in Figure 3a are masked by a strong background. One may therefore wonder, whether a particular data processing method could improve the sharpness of the peaks. In the literature, different procedures have already been used, but they have not carefully been compared with each other. In forming histograms, the proposed procedures consist of (a) disregarding $G(z)$ -curves that do not present clear plateaus,^{16,27} (b) only using data points that belong to plateaus, instead of taking the whole $G(z)$ data,²⁰ (c) only using average values derived from the data points belonging to conductance plateaus, and weighting these by the plateau length;¹⁷ and d) using conductance jumps.¹⁸ In focusing on the plateau values, these methods do effectively eliminate a background. However, they can be subjective, as they involve decisions as how constant the signal has to be to define a plateau, or where the plateau exactly starts and ends.

We propose here an alternative method, which does not make use of any data selection. We take all data, and only subtract a background that is adapted to the physics of the problem. This method is as powerful as all the previous ones and, most importantly, it is fully objective. In proceeding, we note that the conductance must contain a tunneling contribution.²⁴ The tunneling conductance G is exponentially dependent on the gap distance d , i.e., $G \propto \exp(-2\kappa d)$. Here, $\kappa = \sqrt{2m\phi}/\hbar$ is the decay constant, ϕ the apparent barrier height, and m the electron mass. Furthermore, $d = a(z - z_0)$, where a is the attenuation factor of the MCBJ,^{24,25} and z_0 is defined as $z(d = 0)$. Rewriting this, we find $\ln G = -2\kappa a z + \text{constant}$. It seems therefore much more appropriate to plot histograms of $\ln G$ rather than of G .

Making use of this expression, we can now calculate which is the expected tunneling contribution in the conductance histograms. If we denote with N_G , $N_{\ln G}$, and N_z the respective probabilities of measuring a certain value of G , $\ln G$ and z , we may write

$$N_G(G) dG = N_{\ln G}(\ln G) d \ln G = -N_z(z) dz. \quad (1)$$

Here, $N_z(z) = R/v_z$, where R is the data acquisition rate, and v_z is the velocity of the vertical push-rod. In our case, both these quantities are constant: $R = 500$ points/s, $v_z = 30 \mu\text{m/s}$. Solving eq 1 for $N_{\ln G}$ yields

$$N_{\ln G}(\ln G) = \frac{R}{2 v_z \kappa a}. \quad (2)$$

Consequently, $N_{\ln G}$ is constant, whenever ϕ and a are constants. Hence, in a $\ln G$ - or $\log G$ -histogram, tunneling shows up as a constant background which is easily subtracted. In Figure 3b, we show a $\log G$ -histogram built from the data in Figure 3a (bin size: $\Delta \log(G/G_0) = 5 \times 10^{-3}$). A constant background is indeed present for $G \lesssim 2 \times 10^{-4} G_0$ for the pure solvent (blue line), for which tunneling is the only expected contribution. In contrast, clear peaks appear in the presence of octanedithiol. The $\log G$ -histogram representation is very powerful for another reason: it presents a full overview of the data. At a glance, both the single-atom Au contact peaks ($G \approx G_0$) and the

molecules signal ($G < 10^{-3} G_0$) are seen. Between 10^{-2} – $10^{-3} G_0$ (depending on the sample) and G_0 , there is almost no weight in the histograms. This indicates that the Au atoms retract quickly immediately after breaking the gold atom bridge.

The tunneling background, which is constant in a log G -histogram, is inversely proportional to G in a G -histogram, the latter being the representation the literature focused on so far. Solving eq 1 for N_G yields

$$N_G(G) = \frac{R}{2v_z\kappa a} \frac{1}{G}. \quad (3)$$

As can be seen in Figure 3a, this expression perfectly matches the G -histogram of the pure solvent. The blue-line backgrounds of Figure 3a and b correspond to the same $R/(2v_z\kappa a)$.

We can use this property to subtract the tunneling background for the histograms on dithiol molecules. To this end, we fit eq 3 to our data from below. This background is shown in Figure 3a (black-dashed line). The same $R/(2v_z\kappa a)$ gives the black-dashed constant background in Figure 3b. Subtracting it from the data yields a corrected histogram which is guided by the physics of tunneling. The result of this subtraction is shown in gray in Figure 4 (main panel and insets), for two different samples. Figure 4a corresponds to the data of Figure 3. From this analysis we conclude that junctions with conductance values at multiples of $4.5 \times 10^{-5} G_0$ are more favorably formed. This number is then assigned to the conductance of a single Au-octanedithiol-Au bridge, G_1 .

We will next compare our background subtraction method with other approaches based on curve selection. This comparison is shown in Figure 4. The blue-line histogram has been obtained by taking only curves in which plateaus are apparent (i.e. the blue and red curves in Figure 2). In the red dashed histogram only the points within a plateau have been used. The latter data selection scheme is highlighted in black in Figure 2. The selection was done manually and no other treatment was applied.

On comparison of these three histograms, it is quite striking that all exhibit the same key

features. There are two, sometimes even three conductance peaks at multiples of the same G -value (i.e., $G_1 \approx 4.5 \times 10^{-5} G_0$). Particularly interesting is that the gray and blue-line histograms in Figure 4 are almost identical. One can conclude from this that the $G(z)$ curves without apparent plateaus can, on average, be described by a tunneling dependence. The effective barrier height in this case is somewhat smaller than that in the pure solvent. The third, red-dashed histogram, in which only plateau values were considered also yields similar peak positions, but appears to have an even stronger background subtracted. This is expected as in this histogram the noisy signals away from the plateaus (as shown in the red curves of Figure 2) have been removed.

From the histograms, we find a single molecule conductance $G_1 \approx 4.5 \times 10^{-5} G_0$. In literature, values ranging from 1 to $25 \times 10^{-5} G_0$ have been reported.^{1,3,17-21} Our value lies very close to the one found by Wandlowski et al.²⁰ It is also close to that of Steigerwald et al.²⁸ for octanediamine in trichlorobenzene ($2 - 6 \times 10^{-5} G_0$), which was obtained without the need of any data selection. This similarity is particularly remarkable considering the different bonding group of the molecules. Tao et al.¹⁷ reported two groups of peaks, at multiples of $G_L = 5.2 \times 10^{-5} G_0$ and multiples of $G_H = 2.5 \times 10^{-4} G_0$. They attributed these to two distinct microscopic arrangements of the molecule-S-Au bonds. Whereas the first value agrees well with our findings, we do not observe any other peak at higher conductance values. This is especially made clear by the log G -histogram of Figure 3b. The different solvent used in their work could be a possible cause for the formation of the second group of peaks. However, Tao et al.¹⁷ observed peaks at the same conductance values in different solvents. Another notable difference between the two experiments is the speed at which the junctions are opened: 40 nm/s in the work of Tao et al.,¹⁷ and 1 nm/s in our case. We speculate that the change in speed could lead to the detection of different microscopic conformations. Finally, a given microscopic arrangement could also be favored in our symmetric MCBJ, in comparison with the more asymmetric junctions formed in a scanning tunneling microscopy (STM) configuration.

From the above discussion, it is clear that a detailed analysis of conductance histograms is

required to gain insight in the microscopic formation of single molecule junctions. In the analysis methods employed so far, a data selection process has been used. In contrast, we demonstrate that a simple background subtraction scheme suffices. It is as powerful as any data selection scheme and, in contrast to the latter, it is objective. We emphasize that the statistical analysis is most conveniently performed in a histogram in which $\log G$ is represented. The $\log G$ representation allows a simple background subtraction and provides an overview from the single atom contact to tunneling. Moreover, the single (few) molecule conductance values show up in a much more striking manner. In addition, we conclude that the features appearing in the conductance histograms obtained with break junctions (in MCBJ or STM configuration) are robust and can be realistically attributed to the molecular signature in these junctions.

We thank Th. Wandlowski for fruitful discussions and M. Steinacher for technical support. S.J.vd.M. acknowledges the Netherlands Organisation for Scientific Research, NWO ('Talent stipendium'), and M.T.G. the "Ministerio de Educación y Ciencia", for financial support. This work is supported by the Swiss National Center of Competence in Research "Nanoscale Science", the Swiss National Science Foundation, and the European Science Foundation through the Euro-core program on Self-Organized Nanostructures (SONS).

Supporting Information Available: Experimental details. This material is available free of charge via the Internet at <http://pubs.acs.org>.

References

1. Cui, X. D.; Primak, A.; Zarate, X.; Tomfohr, J.; Sankey, O. F.; Moore, A. L.; Moore, T. A.; Gust, D.; Harris, G.; Lindsay, S. M. *Science* **2001**, *294*, 571-574.
2. Donhauser, Z. J.; Mantooth, B. A.; Kelly, K. F.; Bumm, L. A.; Monnell, J. D.; Stapleton, J. J.; Price Jr., D. W.; Rawlett, A. M.; Allara, D. L.; Tour, J. M.; Weiss, P. S. *Science* **2001**, *292*, 2303-2307.
3. Xu, B.; Tao, N. J. *Science* **2003**, *301*, 1221-1223.
4. Agrait, N.; Yeyati, A. L.; van Ruitenbeek, J. M. *Physics Reports* **2003**, *377*, 81-279.
5. Reed, M. A.; Zhou, C.; Muller, C. J.; Burgin, T. P.; Tour, J. M. *Science* **1997**, *278*, 252-254.
6. Smit, R. H. M.; Noat, Y.; Untiedt, C.; Lang, N. D.; van Hemert, M. C.; van Ruitenbeek, J. M. *Nature* **2002**, *419*, 906-909.
7. Reichert, J.; Ochs, R.; Beckmann, D.; Weber, H. B.; Mayor, M.; v. Löhneysen, H. *Phys. Rev. Lett.* **2002**, *88*, 176804.
8. Salomon, A.; Cahen, D.; Lindsay, S.; Tomfohr, J.; Engelkes, V. B.; Frisbie, C. D. *Adv. Mater.* **2003**, *15*, 1881-1890.
9. McCreery, R. L. *Chem. Mater.* **2004**, *16*, 4477-4496.
10. Park, J.; Pasupathy, A. N.; Goldsmith, J. I.; Chang, C.; Yaish, Y.; Petta, J. R.; Rinkoski, M.; Sethna, J. P.; Abruña, H. D.; McEuen, P. L.; Ralph, D. C. *Nature* **2002**, *417*, 722-725.
11. Kubatkin, S.; Danilov, A.; Hjort, M.; Cornil, J.; Brédas, J.-L.; Stuhr-Hansen, N.; Hedegård, P.; Bjørnholm, T. *Nature* **2003**, *425*, 698-701.
12. Champagne, A. R.; Pasupathy, A. N.; Ralph, D. C. *Nano Lett.* **2005**, *5*, 305-308.

13. Xu, B.; Xiao, X.; Yang, X.; Zang, L.; Tao, N. *J. Am. Chem. Soc.* **2005**, *127*, 2386-2387.
14. Krans, J. M.; Muller, C.; Yanson, I. K.; Govaert, T. C. M.; Hesper, R.; van Ruitenbeek, J. M. *Phys. Rev. B* **1993**, *48*, 14721-14724.
15. Krans, J. M.; van Ruitenbeek, J. M.; Fisun, V. V.; Yanson, I. K.; de Jongh, L. J. *Nature* **1995**, *375*, 767-769.
16. Xiao, X.; Xu, B.; Tao, N. *J. Nano Lett.* **2004**, *4*, 267-271.
17. Li, X.; He, J.; Hihath, J.; Xu, B.; Lindsay, S. M.; Tao, N. *J. Am. Chem. Soc.* **2006**, *128*, 2135-2141.
18. Haiss, W.; Nichols, R. J.; van Zalinge, H.; Higgins, S. J.; Bethell, D.; Schiffrin, D. J. *Phys. Chem. Chem. Phys.* **2004**, *6*, 4330-4337.
19. Suzuki, M.; Fujii, S.; Fujihira, M. *Jap. J. App. Phys.* **2006**, *45*, 2041-2044.
20. Pobelov, I.; Li, Z.; Wandlowski, T. to be published.
21. Ulrich, J.; Esrail, D.; Pontius, W.; Venkataraman, L.; Millar, D.; Doerrer, L. H. *J. Phys. Chem. B* **2006**, *110*, 2462-2466.
22. Moreland, J.; Ekin, J. W. *J. Appl. Phys.* **1985**, *58*, 3888-3895.
23. van Ruitenbeek, J. M.; Alvarez, A.; Piñeyro, I.; Grahmann, C.; Joyez, P.; Devoret, M. H.; Esteve, D.; Urbina, C. *Rev. Sci. Instrum.* **1996**, *67*, 108-111.
24. Grüter, L.; González, M. T.; Huber, R.; Calame, M.; Schönenberger, C. *Small* **2005**, *1*, 1067-1070.
25. Vrouwe, S. A. G.; van der Giessen, E.; van der Molen, S. J.; Dulic, D.; Trouwborst, M. L.; van Wees, B. J. *Phys. Rev. B* **2005**, *71*, 035313.

26. Weber, H. B.; Reichert, J.; Weigend, F.; Ochs, R.; Beckmann, D.; Mayor, M.; Alrichs, R.; v. Löhneysen, H. *Chemical Physics* **2002**, *281*, 113-125.
27. Xiao, X.; Nagahara, L. A.; Rawlett, A. M.; Tao, N. *J. Am. Chem. Soc.* **2005**, *127*, 9235-9240.
28. Venkataraman, L.; Klare, J. E.; Tam, I. W.; Nuckolls, C.; Hybertsen, M. S.; Steigerwald, M. L. *Nano Lett.* **2006**, *6*, 458-462.

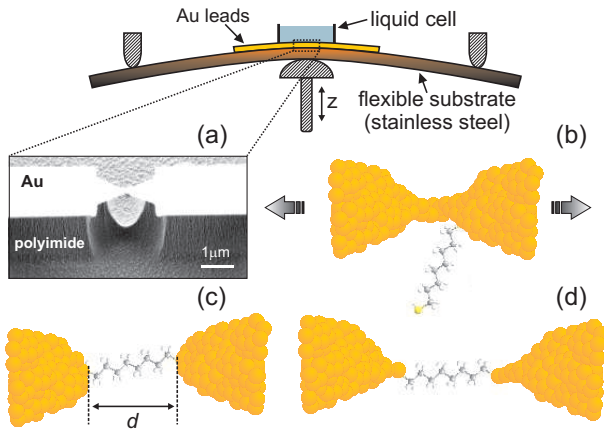


Figure 1: (a) Schematics of the MCBJ principle with liquid cell and a SEM image of one underetched Au junction. (b)-(d) Principle of the formation of a metal-molecule-metal bridge during the breaking process. Starting from the fused Au leads (b), a molecule can lock between the leads (c). Under further stretching, the Au leads are deformed, while the Au-octanedithiol-Au junction stays intact (d).

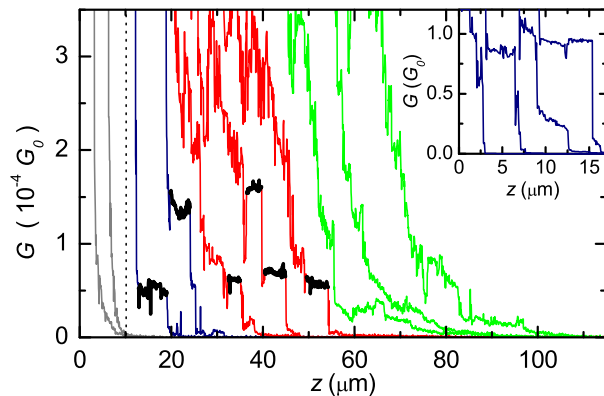


Figure 2: Variation of conductance during the breaking process of a junction in pure mesitylene (left of the vertical pointed line), and in a solution of octanedithiol in mesitylene (right). The curves are shifted in z for clarity. In the presence of octanedithiol, 50 % of the curves present plateaus. From these, some are very clean (the two first ones from left - blue), and others are noisier (the following three ones - red). The remaining 50 % (the last three ones - green) show an irregular decay without plateaus. The plateaus have been highlighted in black. Inset: Examples of plateaus close to $1 G_0$, corresponding to one-atom gold contacts.

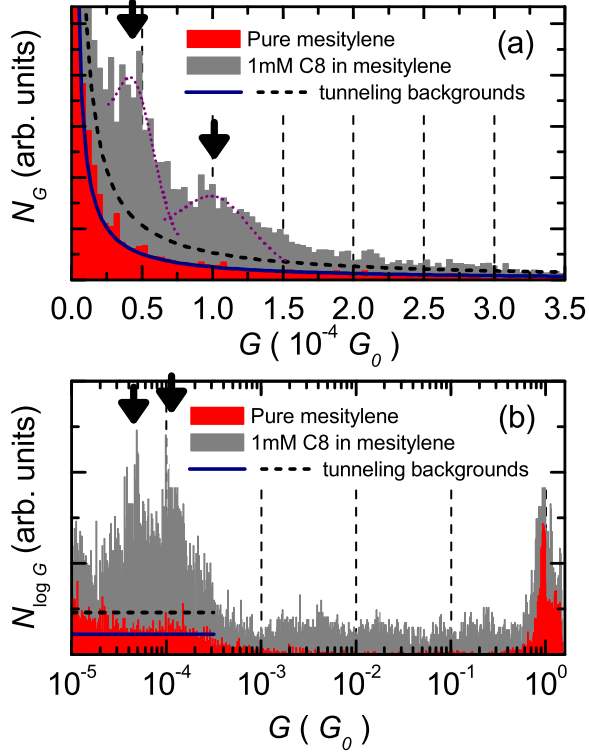


Figure 3: (a) Conductance histograms built from approximately 100 $G(z)$ curves (Figure 2) in pure mesitylene (red), and in a solution 1mM of octanedithiol (grey). The arrows indicate the conductance peaks that appear when octanedithiol is added in solution. The blue and black-dashed lines show the best fit from below using a expression $\propto 1/G$ to both histograms.(b) Histograms of $\log G$ built from the same data as in (a). The blue and black-dashed lines correspond to the same $R/(2v_z\kappa a)$ values as in (a). Note that in the latter representation both atomic gold peaks and molecular peaks are observed.

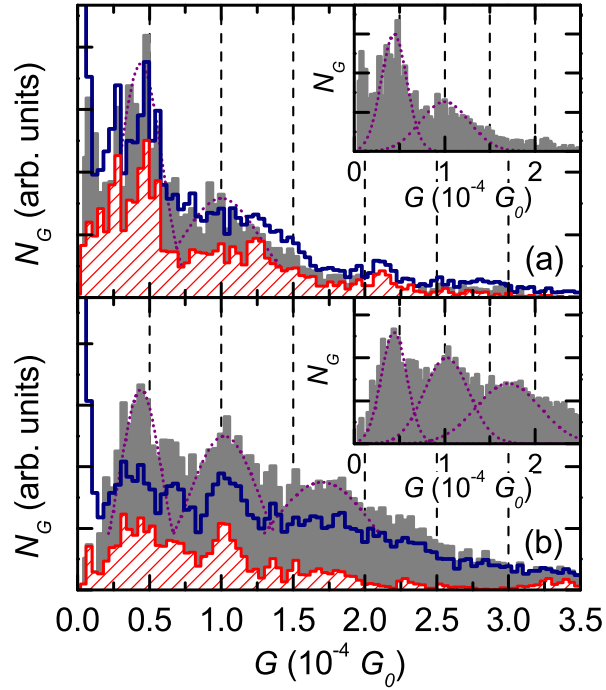


Figure 4: Histograms built from a given group of $G(z)$ curves. (a) and (b) show results for two different samples. The grey histograms were obtained considering all the measured conductance traces, and subtracting later the tunneling background (also shown in the insets). The blue-line histograms were made with the curves that display clear plateaus (blue and red curves in Figure 2). Finally, the red dashed histograms were built only with the G values which belong to plateaus (marked in thick black in Figure 2). The Gaussian curves highlight the position of the peaks.